Scientific Reports

https://doi.org/10.1038/s41598-026-44718-8

Article in Press

# A novel fractional-order coupled model integrating a damped oscillator equation with a non-Fickian heat conduction equation

Received: 12 January 2026

Accepted: 13 March 2026

Published online: 19 March 2026

Cite this article as: Li T., Zhao X., Zhang Y. *et al.* A novel fractional-order coupled model integrating a damped oscillator equation with a non-Fickian heat conduction equation. *Sci Rep* (2026). https://doi.org/10.1038/s41598-026-44718-8

Tongxing Li, Xiaodong Zhao, Yongfeng Zhang, Yan Wang & Yuqing Hu

We are providing an unedited version of this manuscript to give early access to its findings. Before final publication, the manuscript will undergo further editing. Please note there may be errors present which affect the content, and all legal disclaimers apply.

If this paper is publishing under a Transparent Peer Review model then Peer Review reports will publish with the final article.

ARTICLE IN PRESS

© The Author(s) 2026. **Open Access** This article is licensed under a Creative Commons Attribution-NonCommercial-NoDerivatives 4.0 International License, which permits any non-commercial use, sharing, distribution and reproduction in any medium or format, as long as you give appropriate credit to the original author(s) and the source, provide a link to the Creative Commons licence, and indicate if you modified the licensed material. You do not have permission under this licence to share adapted material derived from this article or parts of it. The images or other third party material in this article are included in the article's Creative Commons licence, unless indicated otherwise in a credit line to the material. If material is not included in the article's Creative Commons licence and your intended use is not permitted by statutory regulation or exceeds the permitted use, you will need to obtain permission directly from the copyright holder. To view a copy of this licence, visit http://creativecommons.org/licenses/by-nc-nd/4.0/.

ARTICLE IN PRESS

# Fractional-Order Coupled Model of Damped Oscillator and Heat Conduction

**Tongxing Li[1,*], Xiaodong Zhao[1], Yongfeng Zhang[1], Yan Wang[2], and Yuqing Hu[3]**

[1]Taishan University, School of Mathematics and Statistics, Tai'an, 271000, China
[2]Shandong Agricultural University, College of Information Science and Engineering,Tai'an, 271000, China
[3]Jinling Institute of Technology, School of Science, Nanjing, 211100, China
[*]tongxinli@tsu.edu.cn

## ABSTRACT

This paper presents a novel fractional-order coupled model that integrates a damped oscillator equation with a non-Fickian heat conduction equation, tailored to characterize the thermo-mechanical behavior of nanohybrid materials. The model employs time-fractional derivatives to capture the memory effects in viscoelastic damping arising from nanofiller-matrix interactions, while space-fractional derivatives describe anomalous heat transport in hierarchical microstructures. A rigorous theoretical framework is established: the existence and uniqueness of solutions are proven via the Banach fixed-point theorem, and uniform stability in the $L_2$ sense is demonstrated using an energy function method. Furthermore, the dynamic behavior of the system with time delay is systematically investigated, deriving explicit criteria for Hopf bifurcation, including the critical time delay $\theta_c$ and the conditions for supercritical or subcritical bifurcation. Numerical simulations, using the L1 and Grünwald–Letnikov schemes, are conducted to compare the fractional-order model ($\alpha = 0.9$, $\beta = 0.5$) with its integer-order counterpart. The results show that the fractional model preserves more pronounced memory properties and exhibits a slower decay over extended time scales, which is crucial for depicting the long-term dynamic and diffusion characteristics of nanohybrid materials. The proposed framework not only enriches the theoretical system of fractional-order coupled differential equations but also provides a reliable mathematical tool for the dynamic analysis and stability control of thermo-mechanical systems in engineering applications, such as nanocomposite materials and aerospace structures.

**Keywords:** Fractional-order coupled system; Nanohybrid materials; Existence and stability; Hopf bifurcation

ARTICLE IN PRESS

## Introduction

As an emerging mathematical tool, fractional calculus has gained prominence across diverse scientific and engineering domains in recent years. The coupled mathematical model that integrates the fractional-order damped oscillator equation with the heat conduction equation is increasingly recognized as a pivotal framework for studying heat transfer and damped vibration phenomena in complex systems. The development of this model arises from a thorough understanding of the limitations inherent in conventional integer-order models. In many practical contexts, such as thermal diffusion in porous media and the thermo-mechanical response of viscoelastic materials, systems often exhibit memory effects and non-local characteristics. Conventional integer-order models, however, fail to accurately capture these properties. The incorporation of fractional derivatives allows the model to describe more precisely a system's dependence on historical states and spatial inhomogeneities, thereby offering a novel approach for addressing complex thermo-mechanical coupling problems.

A substantial body of scholarly work has focused on the application of fractional derivatives in heat conduction and damped vibration. For example, in the realm of heat conduction, Wyss (1986) conducted foundational research on the time-fractional diffusion equation[1]. By employing the Mellin transform, he derived an analytical solution expressed in terms of the Fox function, laying the groundwork for subsequent studies on fractional the heat conduction equation. Later, Gorenflo (2000) addressed the time-fractional diffusion-wave equation and obtained a scale-invariant solution in the form of the Wright function through the Laplace transform[2]. In damped vibration research, Caputo et al. developed a dissipation model based on fractional differential formulations. Experimental validation demonstrated that this model achieves excellent agreement with the dissipation curves of various materials, including aluminum, copper, glass, silver and steel[3].

Scholars have utilized time-fractional derivative frameworks to capture anomalous diffusion processes that deviate from classical Fickian behavior[4,12,13]. This approach effectively models the inherent memory effects and heavy-tailed characteristics observed in diverse systems. In the context of porous media and mass transfer, studies rigorously investigate non-Fickian transport in porous materials[11,14], establishing time-fractional formalisms as essential tools for quantification and offering fresh interpretations of underlying mechanisms[14]. Specific applications include predicting VOC emissions from wood-based

ARTICLE IN PRESS

panels using a time-fractional mass transfer model and modeling nucleation governed by fractional diffusion[10]. In terms of numerical techniques and image processing, efficient numerical schemes, particularly for variable-order time-fractional advection-diffusion equations, are developed to tackle the computational complexity of these models[4]. Furthermore, fractional-order diffusion models prove effective in practical applications like texture-preserving multiplicative noise removal in image processing, facilitated by fast explicit diffusion solvers[12]. Beyond applications, the established fractional model equations provide a fundamental mathematical basis for describing anomalous diffusion dynamics[13].

Parallel to diffusion studies, research on oscillator dynamics has focused on systems incorporating fractional damping or strong nonlinearities, which are ubiquitous in engineering and physical systems—including those involving nanohybrid materials[17,18]. As advanced new materials with complex microstructures, nanohybrid materials rely on fractional-order non-Fickian diffusion models as a powerful mathematical tool to investigate substance diffusion. Notably, the fractional damping and nonlinear dynamic characteristics central to oscillator dynamics research are inherent in nanohybrid material systems, where complex microstructures induce non-instantaneous damping effects and intricate mass-energy transport behaviors closely associated with fractional-order dynamics and non-Fickian diffusion[19–21].

For fractional damping analysis, novel analytical approaches are introduced specifically for examining damped vibrations in fractional oscillators, offering improved methodologies for understanding their response[5,6,31]. In terms of nonlinear oscillator solutions, the Homotopy Perturbation Method (HPM) is successfully applied to solving complex nonlinear systems, exemplified by its use in analyzing the fractional van der Pol damped oscillator[8]. Moreover, theoretical and simulation studies on coupled systems reveal intricate dynamics in coupled second-order damped oscillators featuring hyperbolic sine nonlinearities. Key findings include the emergence of multistability and the generation of complex attractors, specifically four-scroll chaos, underscoring the profound impact of nonlinear coupling and damping on system evolution[9]. Despite the significant progress achieved in the aforementioned research areas, there remain unresolved challenges in the refinement of fractional models, the development of more efficient numerical algorithms, and the extension of these frameworks to more complex real-world systems[15,16].

This paper presents three key innovations:

1. A unified fractional-order coupled framework is established by integrating the fractional damped oscillator equation with the heat conduction equation. This novel model overcomes the limitations of traditional integer-order approaches in capturing non-local effects and memory-dependent behavior, enabling accurate characterization of complex thermo-mechanical coupling dynamics in real-world systems.

2. A systematic theoretical analysis is conducted to validate the proposed coupled model. Using the Banach fixed point theorem and an energy function-based approach, we rigorously prove for the first time, the existence, uniqueness, and uniform stability of solutions in the $L_2$ sense, thereby laying a solid theoretical foundation for the model's reliability and applicability.

3. The dynamic behavior of the fractional-order coupled system with time delay is thoroughly investigated. Explicit criteria are derived for Hopf bifurcation, including the critical time delay, bifurcation direction, and stability of emerging periodic solutions. This work reveals the intricate regulatory role of time delay in system dynamics, offering new theoretical insights for stability control in engineering applications.

This paper proposes a novel coupled mathematical model by integrating the fractional-order damped oscillator equation with the fractional heat conduction equation, which is suitable for characterizing the thermo-mechanical coupling and multi-physics behaviors of nanohybrid materials. Compared with recent review articles on fractional-order modeling in materials science, the present work provides several distinct and novel contributions. First, most existing reviews focus on separate applications of fractional calculus in either material diffusion or structural dynamics, whereas this paper establishes a unified coupled system that simultaneously captures memory-dependent damping and non-Fickian transport, which is essential for describing complex dynamic processes in advanced materials. Second, while many reviews only summarize numerical simulations and qualitative properties, this study presents a rigorous theoretical analysis including the existence, uniqueness, and uniform stability of solutions via the Banach fixed-point theorem and energy estimates in the $L^2$ sense. Third, in contrast to existing surveys that rarely address time-delay effects, this work systematically investigates delay-induced Hopf bifurcation in the fractional coupled system, deriving the critical time delay, bifurcation direction, and stability conditions for periodic solutions.

The proposed model overcomes the limitations of traditional integer-order models in capturing memory effects and non-local characteristics, and extends the application scope of fractional calculus to coupled thermo-mechanical systems. The theoretical results show that the fractional-order system possesses strong memory properties and slower energy decay, which is of great significance for depicting the long-term dynamic and diffusion behaviors of nanohybrid materials. Numerical simulations further verify the effectiveness of the model and demonstrate the influences of fractional orders, coupling coefficients, and time delay on system responses.

This study not only enriches the theoretical system of fractional-order coupled differential equations but also provides a reliable mathematical tool for the dynamic analysis and stability control of thermo-mechanical systems in engineering applications, such as nanocomposite materials, aerospace structures, and vibration-heat coupling systems. Future work will

ARTICLE IN PRESS

focus on the development of more efficient numerical algorithms, the experimental calibration of model parameters, and the extension of the proposed framework to more complex multi-field coupling problems with variable fractional orders.

The paper is organized as follows. Section 1 provides the introduction. The fractional-order model is developed in Section 2. The existence and uniqueness of the solution are established in Section 3, followed by a proof of its uniform stability in Section 4. Section 5 theoretically examines the bifurcation behavior of the fractional-order delayed model. Numerical examples are presented in Section 6, and the paper concludes with a summary in Section 7.

## Model Analysis

Firstly, the parameter assumptions used throughout the paper are given.

**Assumptions 1.** The Caputo fractional derivative definition is given by

$$D_t^{\alpha}u(t,x) = \frac{1}{\Gamma(1-\alpha)}\int_0^t \frac{1}{(t-\tau)^{\alpha}}\frac{\partial u(\tau,x)}{\partial \tau}d\tau, \tag{1}$$

$$D_x^{\beta}u(t,x) = \frac{1}{\Gamma(1-\beta)}\int_0^x \frac{1}{(x-\tau)^{\beta}}\frac{\partial u(t,\tau)}{\partial \tau}d\tau, \tag{2}$$

where $\alpha \in (0,1)$ denotes the order of the time-fractional derivative; $\Gamma(\cdot)$ is the Gamma function, defined as $\Gamma(z) = \int_0^{\infty} t^{z-1}e^{-t}dt$. The time domain $t \in [0,T]$ and the spatial domain $x \in [0,L]$, the boundary conditions are Dirichlet conditions $u(t,0) = u(t,L) = 0$. $f(t,x)$ is a source term used to introduce external stimuli or material energy inputs. $T > 0$ is the upper bound of time, $\Omega$ represents the spatial domain. The space $X$ is a complete metric space that satisfies the requirement of Banach's theorem for spatial completeness.

This study investigates a mathematical model that couples the fractional-order damped oscillator equation with the heat conduction equation, and its formula is as follows:

$$D_t^{2\alpha}u(t,x) + \frac{1}{2}D_t^{\alpha}u(t,x) + u(t,x) = kD_x^{\beta}u(t,x) + f(t,x), \tag{3}$$

where $D_t^{2\alpha}u(t,x)$ represents the fractional-order acceleration term, and $\frac{1}{2}D_t^{\alpha}u(t,x)$ represents the fractional-order damping term, which compared to the integer order damping term, can more flexibly describe the damping characteristics of the system and capture the energy dissipation process at different time scales. $u(t,x)$ is the state variable of the system, which can denotes physical quantities such as displacement, concentration and temperature. The $kD_x^{\beta}u(t,x)$ on the right-hand side of the equation denotes the heat conduction term, when $\beta = 2$, the equation corresponds to the classical heat conduction equation, which describes the diffusion behavior of physical quantities in space.

In the following, based on the Banach fixed point theorem, we prove the existence and uniqueness of solutions to the coupled equation of fractional order damped oscillators and the heat conduction. We need to use Riemann-Liouville(RL) fractional integral, which is defined as follows

$$I_t^{\alpha}v(t,x) = \frac{1}{\Gamma(\alpha)}\int_0^t \frac{v(\tau,x)}{(t-\tau)^{1-\alpha}}d\tau, \tag{4}$$

$I_t^{\alpha}$ is the right inverse of $D_t^{\alpha}$, which means that when $v(0,x) = 0$, then $D_t^{\alpha}I_t^{\alpha}v = v$ is satisfied. Taking the Banach space $X = C([0,T];L_2(\Omega))$ as the spatial region. The norm in its space is defined as:

$$\|u\|_X = \sup_{t\in[0,T]} \|u(t,\cdot)\|_{L^2(\Omega)},\ \|v\|_{L^2(\Omega)} = \left(\int_{\Omega}|v(x)|^2dx\right)^{\frac{1}{2}}. \tag{5}$$

**Remark 1.** As $\alpha$ decreases, the memory effect of the system strengthens, and the temporal non-locality becomes more pronounced. By adjusting $\alpha$, the differences in the temporal characteristics of damping and diffusion processes across various practical systems can be accommodated. $\beta$ denotes the order of the space-fractional derivative. When $\beta = 2$, it corresponds to the classical Fickian diffusion. If the value of $\beta$ deviates from 2, it can be used to describe non-Fickian diffusion phenomena. For instance, in porous media, the diffusion of substances may not follow the traditional second-order diffusion law due to the fractal structure of the medium or its complex pore morphology. The $k$ determines the diffusion rate of physical quantities in space, and its numerical value is closely related to the properties of the medium. As an external input, $f(t,x)$ directly determines the excitation characteristics of the system through its form and value.

**Remark 2.** Although the proposed fractional-order model appears mathematically abstract, it is physically rooted in the thermo-mechanical behavior of nanohybrid materials. The time-fractional derivative describes power-law viscoelastic damping arising from nanofiller-matrix interactions. The space-fractional derivative characterizes non-Fickian heat transport in porous

ARTICLE IN PRESS

and hierarchical microstructures. The time delay represents thermal relaxation, energy exchange lag, and diffusive latency observed in real nanocomposites. Thus, every component of the model corresponds to a measurable physical mechanism in nanohybrid materials, rather than being a purely theoretical construct. This physical mapping is rigorously established in the literature, where fractional calculus is widely recognized as the natural framework for modeling memory-dependent damping and non-local transport in nanohybrid materials[22].

**Remark 3.** A concrete physical realization of the proposed model is the epoxy-graphene nanocomposite (a typical nanohybrid material), with all model parameters calibrated against experimental data from dynamic mechanical analysis (DMA) and laser flash analysis (LFA)[22,27]. Epoxy resin reinforced with 0.5 wt% graphene nanoplatelets (GNPs), used in aerospace thermal-mechanical components[23]. Fractional order $\alpha = 0.88$, corresponding to the power-law viscoelastic damping of the nanocomposite, measured via DMA at $25°C$ (loss tangent $\tan\delta = 0.43$, storage modulus $E' = 3.4$ GPa), Space-fractional order $\beta = 0.47$. Characterizing non-Fickian thermal diffusion in the composite's hierarchical microstructure (pore size 50–200 nm), with thermal diffusivity $\kappa = 0.82$ W/m·K measured via LFA[26]. Coupling coefficient $k = 1.05$, scaled to the thermo-mechanical coupling factor ($\lambda = 1.18 \times 10^{-4} K^{-1}$) of the epoxy-graphene nanocomposite[27]. Time delay $\theta = 0.78$ s, corresponding to the thermal relaxation time of the nanocomposite, induced by phonon scattering at graphene-epoxy interfaces[25,26]. External excitation $f(t,x) = 50\sin(10t)$ MPa, typical cyclic thermal-mechanical loading in aerospace applications[24]. This parameter set is fully grounded in experimental observations of epoxy-graphene nanocomposites, confirming the model's physical relevance.

## Existence and uniqueness of solutions

By leveraging the inverse properties of fractional-order integration and differentiation, the original equation (3) can be transformed into an integral equation[28,29]. From (3), it is clear that

$$D_t^{2\alpha}u(t,x) = kD_x^{\beta}u(t,x) - u(t,x) - \frac{1}{2}D_t^{\alpha}u(t,x) + f(t,x), \tag{6}$$

$$I_t^{2\alpha}D_t^{2\alpha}u(t,x) = u(t,x) = I_t^{\alpha}\left[I_t^{\alpha}(kD_x^{\beta}u(t,x) - u(t,x) - \frac{1}{2}D_t^{\alpha}u(t,x) + f(t,x))\right]. \tag{7}$$

In the following, this paper gives an important theorem.

**Theorem 1.** The solution to the original equation (3) exists and is unique.

Based on this integral equation, for any $u \in X$, a mapping $F : X \to X$ can be constructed as,

$$(Fu)(t,x) = I_t^{\alpha}\left[I_t^{\alpha}(kD_x^{\beta}u(t,x) - u(t,x) - \frac{1}{2}D_t^{\alpha}u(t,x) + f(t,x))\right], \tag{8}$$

obviously, the solution to the original equation is equivalent to a fixed point of $F$, that is to say, $u$ satisfies the equation $Fu = u$. By utilizing the boundedness of fractional integrals, the Riemann-Liouville fractional integral $I_t^{\alpha}g(t)$ satisfies

$$\|I_t^{\alpha}g(t)\|_{L^p([0,T])} \le C_{\alpha,p}T^{\alpha}\|g(t)\|_{L^q([0,T])}, \tag{9}$$

where $C_{\alpha,p}$ is a constant, $p$ and $q$ satisfying the Sobolev embedding conditions for fractional integration[28] . Assuming that fractional differential operators $D_t^{\alpha}$, $D_x^{\beta}$ are bounded, then there exist constants $M_1, M_2$ such that for any $u \in X$, we have

$$\|D_t^{\alpha}u\|_X \le M_1\|u\|_X, \|D_x^{\beta}u\|_X \le M_2\|u\|_X. \tag{10}$$

For any $u_1, u_2 \in X$, let $w = u_1 - u_2$, then $Fu_1 - Fu_2 = I_t^{\alpha}\left[I_t^{\alpha}(kD_x^{\beta}w - w - \frac{1}{2}D_t^{\alpha}w)\right]$. By utilizing the boundedness of fractional integrals and estimating the norm of time integrals, we can obtain

$$\|I_t^{\alpha}(kD_x^{\beta}w - w - \frac{1}{2}D_t^{\alpha}w)\|_{L^2([0,t];L^2(\Omega))} \le C_{\alpha}T^{\alpha}(|k|M_2 + 1 + \frac{1}{2}M_1)\|w\|_X, \tag{11}$$

and

$$\left\|I_t^{\alpha}\left[I_t^{\alpha}(kD_x^{\beta}w - w - \frac{1}{2}D_t^{\alpha}w)\right]\right\|_{L^2([0,t];L^2(\Omega))} \le C_{\alpha}^2T^{2\alpha}(|k|M_2 + 1 + \frac{1}{2}M_1)\|w\|_X, \tag{12}$$

hence, we get

$$\|Fu_1 - Fu_2\|_X \le C_{\alpha}^2T^{2\alpha}(|k|M_2 + 1 + \frac{1}{2}M_1)\|u_1 - u_2\|_X. \tag{13}$$

ARTICLE IN PRESS

If we select a sufficiently small time interval $[0,T]$, we can make

$$L = C_\alpha^2 T^{2\alpha}(|k|M_2 + 1 + \frac{1}{2}M_1) < 1, \tag{14}$$

it is clear that $F : X \to X$ is a contraction mapping[29].

Obviously, $X = C([0,T];L_2(\Omega))$ is a complete space and $F : X \to X$ is a contraction mapping, by using Banach's fixed point theorem. The compressive mapping on a complete metric space must have a unique fixed point $u^* \in X$, which is the solution of the original fractional differential equation, the existence and uniqueness of the equation solution are proved.

**Remark 4.** The assumption that fractional differential operators $D_t^\alpha$ and $D_x^\beta$ are bounded is both mathematically necessary and physically justified. Mathematically, this boundedness (i.e., $\|D_t^\alpha u\|_X \le M_1\|u\|_X$ and $\|D_x^\beta u\|_X \le M_2\|u\|_X$ for constants $M_1, M_2 > 0$) is a critical technical condition for deriving the contraction mapping estimate $\|Fu_1 - Fu_2\|_X \le L\|u_1 - u_2\|_X$ required in the Banach fixed-point theorem—without it, the norm bounds for fractional derivative terms in the integral equation cannot be rigorously established, and the contraction property would fail to hold. Physically, this assumption aligns with the finite nature of real-world processes in nanohybrid materials, $D_t^\alpha$ characterizes memory-dependent damping (with finite energy dissipation) and $D_x^\beta$ describes non-Fickian diffusion (with finite spatial transport intensity), neither of which can be unbounded in practical material systems.

**Remark 5.** In the above contraction mapping argument, the smallness condition imposed on the time horizon $T$ is essential. The Lipschitz constant $L = C_\alpha^2 T^{2\alpha}(|k|M_2 + 1 + \frac{1}{2}M_1)$ depends polynomially on $T^{2\alpha}$, so $L$ can be made strictly less than 1 if and only if $T$ is sufficiently small. This means that the existence and uniqueness result obtained above is a local-in-time result,valid on some small interval $[0,T]$ where the contraction condition $L < 1$ holds. By the standard method of continuation of solutions for fractional differential equations, one may iteratively extend the unique local solution to longer time intervals as long as the solution remains in the function space $X$ and the boundedness assumptions on the fractional operators remain valid. Thus, the solution can be extended to a maximal existence interval, and in typical dissipative systems under energy estimates, global-in-time existence and uniqueness can be further established.

**Remark 6.** The contraction condition $L = C_\alpha^2 T^{2\alpha}\left(|k|M_2 + 1 + \frac{1}{2}M_1\right) < 1$ relies crucially on the factor $T^{2\alpha}$, which can be made arbitrarily small by reducing $T$. First, it controls the double fractional integral $\|I_t^\alpha I_t^\alpha(\cdot)\|_{L^2([0,T];L^2(\Omega))} \le C_\alpha^2 T^{2\alpha}\|\cdot\|_X$, which is the source of the factor $T^{2\alpha}$. Second, it ensures that the combined influence of the spatial fractional operator $kD_x^\beta$, the damping term $\frac{1}{2}D_t^\alpha$, and the potential term $u$ remains dominated by the contraction induced by small time. Thus the smallness of $T$ is not used to restrict $k$, but rather to compensate for the combined magnitude of $|k|M_2 + 1 + \frac{1}{2}M_1$. Accordingly, the local existence and uniqueness result does not require $k$ to be small; it holds for any fixed $k \in \mathbb{R}$, provided $T$ is chosen sufficiently small depending on $|k|$. In other words, for any bounded $k$, one can always find a short enough time interval $[0,T]$ on which the contraction mapping argument applies. If one further imposes a smallness condition on $|k|$ together with energy estimates as in the stability analysis, the solution can be extended globally in time, and the range of admissible values of $k$ can be explicitly quantified via the constants in the dissipative estimates.

## Stability analysis of solutions

The uniform stability of solutions to the differential equations coupling the fractional-order damped oscillator equation and the heat conduction equation serve as a prerequisite for the safe operation of the system, which is prevalent in such fields as aerospace engineering and mechanical structures.

First, we clarify how the uniform stability of the solution to the equation is defined in the sense of $L_2$. It is assumed that a solution is said to be uniformly stable if there exists a constant $M > 0$ such that for any initial value $(u_0, v_0)$ and nonhomogeneous term $f$,for $t \in [0,T]$, the solution of the equation satisfies

$$\|u(t,x)\|_{L^2}^2 + \|D_t^\alpha u(t,x)\|_{L^2}^2 \le M\left(\|u_0(x)\|_{L^2}^2 + \|v_0(x)\|_{L^2}^2 + \int_0^t \|f(s,x)\|_{L^2}^2 ds\right). \tag{15}$$

This paper presents the second important theorem in the following.

**Theorem 2.** The solution to the original equation (3) is uniformly stable in the $L_2-$sense.

In order to prove the uniform stability of the solution, we make the following assumptions. It is assumed that $\alpha \in (0,1)$, $\beta \in [0,2\alpha]$, $u_0(x), v_0(x) \in L^2(\Omega)$, $u(0,x) = u_0(x)$, $D_t^\alpha u(0,u) = v_0(x)$, $u(t,0) = u(t,L) = 0$, $k$ is a constant that satisfies the small perturbation condition $|k| < C$, $0 < C \ll 1$, assuming $f(t,x)$ is a function with finite energy and satisfies $f(t,x) \in L^2([0,T]\times\Omega)$.

Define the $L^2-$norm of the energy function $E(t)$, which includes the solution and its first-order fractional derivative,

$$E(t) = \frac{1}{2}\|D_t^\alpha u(t,x)\|_{L^2}^2 + \frac{1}{2}\|u(t,x)\|_{L^2}^2,\ \|g(t,x)\|_{L^2}^2 = \int_\Omega [g(t,x)]^2 dx. \tag{16}$$

ARTICLE IN PRESS

Where $\|D_t^\alpha u(t,x)\|_{L^2}^2$ denotes the fractional-order kinetic energy and $\|u(t,x)\|_{L^2}^2$ presents the potential energy. Differentiate $E(t)$ with respect to $t$, using the product rule for differentiation, the property $\frac{d}{dt}\|g(t,x)\|_{L^2}^2 = 2\int_\Omega g(t,x)\frac{\partial g(t,x)}{\partial t}dx$ of the Caputo derivative and the semigroup properties of fractional derivatives, we can obtain

$$\begin{aligned}\frac{dE(t)}{dt} &= \int_\Omega D_t^\alpha u(t,x)\frac{\partial}{\partial t}D_t^\alpha u(t,x)dx + \int_\Omega u(t,x)\frac{\partial u(t,x)}{\partial t}dx = \int_\Omega D_t^\alpha u(t,x)D_t^\alpha\frac{\partial u(t,x)}{\partial t}dx + \int_\Omega u(t,x)\frac{\partial u(t,x)}{\partial t}dx,\\ &= \int_\Omega D_t^\alpha u(t,x)D_t^{2\alpha}u(t,x)dx + \int_\Omega u(t,x)\frac{\partial u(t,x)}{\partial t}dx. \end{aligned} \tag{17}$$

By expressing $D_t^{2\alpha}u(t,x)$ from the original equation (3) and moving all nonsecond-order derivative terms to the right-hand side of the equation, we can obtain

$$D_t^{2\alpha}u(t,x) = kD_x^\beta u(t,x) + f(t,x) - \frac{1}{2}D_t^\alpha u(t,x) - u(t,x). \tag{18}$$

Substituting (18) into the first term of (17) and splitting the integral, we have

$$\frac{dE(t)}{dt} = \int_\Omega [D_t^\alpha u\cdot(kD_x^\beta u - \frac{1}{2}D_t^\alpha u - u) + D_t^\alpha u\cdot f]dx + \int_\Omega u\cdot\frac{\partial u}{\partial t}dx, \tag{19}$$

To facilitate the subsequent estimation of equation (19), we denote

$$I_1 = \int_\Omega D_t^\alpha u\cdot(kD_x^\beta u - \frac{1}{2}D_t^\alpha u - u)dx,\ I_2 = \int_\Omega D_t^\alpha u\cdot f dx,\ I_3 = \int_\Omega u\cdot\frac{\partial u}{\partial t}dx, \tag{20}$$

respectively.

Then, we have

$$\frac{dE(t)}{dt} = I_1 + I_2 + I_3. \tag{21}$$

**Theorem 3.** Using the core properties of the Caputo fractional derivative, for any function $u\in C^1([0,T];L^2(\Omega))$ satisfying the homogeneous boundary condition $u(t,0)=u(t,L)=0$ with $\alpha\in(0,1)$, we have the integral identity

$$\int_\Omega u\cdot\frac{\partial u}{\partial t}dx = \int_\Omega D_t^\alpha u\cdot D_t^{2\alpha-1}u dx, \tag{22}$$

between the fractional derivative and the partial derivative with respect to time holds true.

For $\gamma\in(-1,0)$, the RL fractional derivative of order $\gamma$ is defined as the RL fractional integral of order $-\gamma$, then

$$D_t^\gamma u(t,x) = I_t^{-\gamma}u(t,x) = \frac{1}{\Gamma(-\gamma)}\int_0^t u(\tau,x)\cdot(t-\tau)^{-\gamma-1}d\tau. \tag{23}$$

For $\gamma = 2\alpha - 1\in(-1,0)$, $\alpha\in(0,1)$, we have $D_t^{2\alpha-1}u = I_t^{1-2\alpha}u$. The derivation relies on two core properties of fractional operators[28,29]. For $u(0,x)=0$ and $\alpha\in(0,1)$, the Caputo derivative and RL integral satisfy

$$I_t^\alpha D_t^\alpha u(t,x) = u(t,x),\ D_t^\alpha I_t^\alpha u(t,x) = u(t,x). \tag{24}$$

For $\gamma_1,\gamma_2>0$, the RL fractional integral satisfies

$$I_t^{\gamma_1}I_t^{\gamma_2}u(t,x) = I_t^{\gamma_1+\gamma_2}u(t,x). \tag{25}$$

The first-order partial derivative can be decomposed into the composition of Caputo derivatives:

$$\frac{\partial u(t,x)}{\partial t} = D_t^1 u(t,x) = D_t^\alpha D_t^{1-\alpha}u(t,x), \tag{26}$$

where $D_t^{1-\alpha}$ is the RL fractional derivative of order $1-\alpha\in(0,1)$.

We now proceed with the derivation of the integral identity, substitute the differential decomposition (26) into the integral $\int_\Omega u(t,x)\cdot\frac{\partial u(t,x)}{\partial t}dx = \int_\Omega u(t,x)\cdot D_t^\alpha D_t^{1-\alpha}u(t,x)dx$.

Under the homogeneous initial condition $u(0,x)=0$, we have $u(t,x) = I_t^\alpha D_t^\alpha u(t,x)$. Then

$$\int_\Omega u(t,x)\cdot\frac{\partial u(t,x)}{\partial t}dx = \int_\Omega I_t^\alpha D_t^\alpha u(t,x)\cdot D_t^\alpha D_t^{1-\alpha}u(t,x)dx. \tag{27}$$

ARTICLE IN PRESS

For the homogeneous Dirichlet boundary condition $u(t,0)=u(t,L)=0$, the spatial integral $\int_\Omega \cdot dx$ commutes with the time-fractional operator $D_t^\alpha$. We thus rewrite the integral (27) as,

$$\int_\Omega u(t,x)\cdot\frac{\partial u(t,x)}{\partial t}dx=\int_\Omega D_t^\alpha u(t,x)\cdot I_t^\alpha D_t^\alpha D_t^{1-\alpha}u(t,x)dx. \tag{28}$$

By inverse relationship (24) and the semigroup law (25), we have $I_t^\alpha D_t^\alpha D_t^{1-\alpha}u(t,x)=D_t^{1-\alpha}u(t,x)$. For $\alpha\in(0,1)$, $1-\alpha=2\alpha-1+(1-2\alpha)$, and $D_t^{1-2\alpha}=I_t^{2\alpha-1}$ (23). Using the semigroup law again, we get

$$D_t^{1-\alpha}u(t,x)=D_t^{2\alpha-1}I_t^{2\alpha-1}D_t^{1-\alpha}u(t,x)=D_t^{2\alpha-1}u(t,x). \tag{29}$$

Substitute the simplified operator (29) back into the integral (28) to obtain (22), the proof of Theorem 3 is completed.

For the formula (22), the integral can be controlled by applying the Cauchy-Schwarz inequality and the embedding relationship of fractional Sobolev norms, and we have

$$|I_3|\le\|D_t^\alpha u\|_{L^2}\cdot\|D_t^{2\alpha-1}u\|_{L^2}, \tag{30}$$

For any $\varepsilon>0$, it holds that

$$|I_3|\le\frac{\varepsilon}{2}\|D_t^\alpha u\|_{L^2}^2+\frac{1}{2\varepsilon}\|D_t^{2\alpha-1}u\|_{L^2}^2\le\frac{\varepsilon}{2}\|D_t^\alpha u\|_{L^2}^2+\frac{1}{2\varepsilon}C_{\alpha,\Omega}^2\|D_t^{2\alpha-1}u\|_{L^2}^2, \tag{31}$$

Set $\varepsilon=C_{\alpha,\Omega}$, thus, it follows from (31) that $|I_3|\le C_{\alpha,\Omega}\|D_t^\alpha u\|_{L^2}^2$. We decompose $I_1$ into three terms, then $I_1=k\int_\Omega D_t^\alpha u\cdot D_x^\beta u dx-\frac{1}{2}\int_\Omega(D_t^\alpha u)^2dx-\int_\Omega D_t^\alpha u\cdot u dx$. For the first term, by applying the Cauchy-Schwarz inequality, for any $\varepsilon_1>0$, we obtain

$$|k\int_\Omega D_t^\alpha u\cdot D_x^\beta u dx|\le|k|\|D_t^\alpha u\|_{L^2}\cdot\|D_x^\beta u\|_{L^2}\le|k|\left(\frac{\varepsilon_1}{2}\|D_t^\alpha u\|_{L^2}^2+\frac{1}{2\varepsilon_1}\|D_x^\beta u\|_{L^2}^2\right)\le|k|\left(\frac{\varepsilon_1}{2}+C_{\alpha,\beta}^2\frac{1}{2\varepsilon_1}\right)\|D_t^\alpha u\|_{L^2}^2. \tag{32}$$

It is obvious that $-\frac{1}{2}\int_\Omega(D_t^\alpha u)^2dx=-\frac{1}{2}\|D_t^\alpha u\|_{L^2}^2\le0$ is valid. Using inequality estimation techniques similar to those in (32) and for $\varepsilon_2>0$, we can obtain

$$\left|-\int_\Omega D_t^\alpha u\cdot u dx\right|\le\|D_t^\alpha u\|_{L^2}^2\cdot\|u\|_{L^2}^2\le\frac{\varepsilon_2}{2}\|D_t^\alpha u\|_{L^2}^2+\frac{1}{2\varepsilon_2}\|u\|_{L^2}^2, \tag{33}$$

hence

$$|I_1|\le|k|\left(\frac{\varepsilon_1}{2}+C_{\alpha,\beta}^2\frac{1}{2\varepsilon_1}\right)\|D_t^\alpha u\|_{L^2}^2-\frac{1}{2}\|D_t^\alpha u\|_{L^2}^2+\frac{\varepsilon_2}{2}\|D_t^\alpha u\|_{L^2}^2+\frac{1}{2\varepsilon_2}\|u\|_{L^2}^2. \tag{34}$$

For $I_2$ and $\varepsilon_3>0$, we have

$$|I_2|=\left|\int_\Omega D^\alpha u\cdot f dx\right|\le\|D_t^\alpha u\|_{L^2}\cdot\|f\|_{L^2}\le\frac{\varepsilon_3}{2}\|D_t^\alpha u\|_{L^2}^2+\frac{1}{2\varepsilon_3}\|f\|_{L^2}^2. \tag{35}$$

Next, we substitute $I_1$, $I_2$ and $I_3$ into equation (21) respectively, and utilize the definition of the energy function $E(t)=\frac{1}{2}\left(\|D_t^\alpha u\|_{L^2}^2+\|u\|_{L^2}^2\right)$, $\|D_t^\alpha u\|_{L^2}^2\le2E(t)$, $\|u\|_{L^2}^2\le2E(t)$, by selecting appropriate values of $\varepsilon_1$, $\varepsilon_2$ and $\varepsilon_3$ such that the positive coefficient is less than 0.5, the positive coefficient can thus be offset by the negative term, it yields that

$$\begin{aligned}\frac{dE(t)}{dt}&=I_1+I_2+I_3\le\left(\frac{\varepsilon_1|k|}{2}+C_{\alpha,\beta}^2\frac{|k|}{2\varepsilon_1}-\frac{1}{2}+\frac{\varepsilon_2}{2}+\frac{\varepsilon_3}{2}+C_{\alpha,\Omega}\right)\|D_t^\alpha u\|_{L^2}^2+\frac{1}{2\varepsilon_2}\|u\|_{L^2}^2+\frac{1}{2\varepsilon_3}\|f\|_{L^2}^2,\\&\le-C_1E(t)+C_2\|f(t,x)\|_{L^2}^2.\end{aligned} \tag{36}$$

Clearly, the equation (36) is a first-order linear nonhomogeneous differential inequality with respect to $E(t)$, and subsequent proofs can be carried out using the Gronwall inequality. We have $\frac{dE(t)}{dt}+C_1E(t)\le C_2\|f(t,x)\|_{L^2}^2$, it is easy to get $E(t)\le E(0)e^{-C_1t}+C_2e^{-C_1t}\int_0^t\|f(s,x)\|_{L^2}^2e^{C_1s}ds$, using the properties of exponential functions, we further estimate the above inequality and obtain the following bound

$$E(t)\le E(0)+C_2e^{C_1T}\int_0^t\|f(s,x)\|_{L^2}^2ds, \tag{37}$$

ARTICLE IN PRESS

based on the definitions of $E(t)$ and $E(0)$, we thus have

$$\frac{1}{2}\left(\|D_t^{\alpha}u(t,x)\|_{L^2}^2+\|u(t,x)\|_{L^2}^2\right)\leq\frac{1}{2}\left(\|u_0(x)\|_{L^2}^2+\|v_0(x)\|_{L^2}^2\right)+C_2e^{C_1T}\int_0^t\|f(s,x)\|_{L^2}^2ds. \tag{38}$$

Let $M=\max(1,2C_3e^{C_1T})$, then we can rewrite equation (38) to obtain

$$\left(\|D_t^{\alpha}u(t,x)\|_{L^2}^2+\|u(t,x)\|_{L^2}^2\right)\leq M\left(\|u_0(x)\|_{L^2}^2+\|v_0(x)\|_{L^2}^2+\int_0^t\|f(s,x)\|_{L^2}^2ds\right). \tag{39}$$

Apparently, the equation (39) indicates that the solution to the equation is uniformly stable in the $L^2-$sense. The proof of Theorem 2 is completed.

**Remark 7.** $C_{\alpha,\Omega}$ is the embedding constant of the fractional Sobolev space for $D_t^{2\alpha-1}$ into $L^2(\Omega)$ (depending on $\alpha$ and $\Omega$), and $C_{\alpha,\beta}$ is the interpolation constant between $D_t^{\alpha}$ and $D_x^{\beta}$ (depending on $\alpha$ and $\beta$). For the modeled nanohybrid material system, uniform stability in the $L^2$-sense means the state variable $u(t,x)$ and its fractional derivative $D_t^{\alpha}u(t,x)$ are uniformly bounded by initial conditions and external inputs, ensuring stable energy dissipation and non-Fickian diffusion, which is critical for practical engineering reliability.

**Remark 8.** The derivation of the energy inequality employs several standard properties of fractional derivatives and classical inequalities including the Cauchy–Schwarz inequality and Gronwall's inequality.These auxiliary results are well established in the theory of fractional differential equations and functional analysis, and their detailed proofs are omitted here for brevity and readability of the main arguments.

**Remark 9.** The boundary conditions restrict the solution $u(t,x)$ to vanish at the endpoints $x=0$ and $x=L$ for all time $t$. This defines a closed subspace of the Banach space $X=C([0,T];L^2(\Omega))$ consisting of functions that satisfy $u(t,0)=u(t,L)=0$ for every $t\in[0,T]$, ensuring compatibility with the fixed-point argument and energy estimates. A key technical role of the homogeneous Dirichlet conditions is to guarantee that the spatial integral $\int_\Omega\cdot dx$ commutes with the time-fractional differential and integral operators $D_t^{\alpha}$, $I_t^{\alpha}$ in the energy-method derivation. This commutativity is essential for establishing the integral identity in Theorem 3 and for performing integration-by-parts-like estimates in the stability analysis.

## Time delay and bifurcation

In the following, the fractional model (3) with time delay and bifurcation phenomena of solutions is researched. This type of fractional differential equation which is given as,

$$D_t^{2\alpha}u(t,x)+\frac{1}{2}D_t^{\alpha}u(t,x)+u(t-\theta,x)=kD_x^{\beta}u(t,x)+f(t,x). \tag{40}$$

As a prevalent physical phenomenon in practical systems, time delay exerts more complex influence on the dynamical behavior of fractional-order systems. Specifically, time delay may not only destabilize the system but also induce complex dynamical behaviors such as bifurcation and chaos.

The time delay $\theta$ in the proposed fractional-order model possesses clear and distinct physical origins in the thermo-mechanical dynamics of nanohybrid materials.Specifically, it represents thermal relaxation induced by the finite thermal lag and phonon scattering at nanofiller-matrix interfaces; it accounts for feedback mechanisms arising from the non-instantaneous thermo-mechanical coupling between mechanical vibration and temperature-dependent material properties; and it characterizes transport latency associated with non-Fickian heat or mass diffusion through the complex hierarchical microstructure. By unifying these three physically meaningful components, the time delay $\theta$ captures the essential delayed response behavior of the system rather than being a purely mathematical parameter, thereby strengthening the physical rationality of the bifurcation analysis.

The definition of Hopf bifurcation and a lemma are first presented at the beginning of this section.

**Definition 1.** If the stability of the equilibrium solution of the system changes as the parameter $\theta$ crosses its critical value $\theta_c$ , and a periodic solution bifurcates from the equilibrium solution, this phenomenon is referred to as a Hopf bifurcation. For time-delay systems, Hopf bifurcation is typically induced by the eigenvalues crossing the imaginary axis of the complex plane.

**Lemma 1.** Let the characteristic equation of the linear time-delay system be $P(\lambda,e^{-\lambda\theta})=0$. If there exist $\theta=\theta_c>0$ and $\omega>0$ such that $P(i\omega,e^{-i\omega\theta_c})=0$ and $\frac{d}{d\theta}Re(\lambda(\theta_c))\neq0$, then $\theta_c$ is the critical value of Hopf bifurcation.

To analyze the bifurcation phenomenon, we consider the linearized form of the homogeneous equation $(f(t,x)=0)$,

$$D_t^{2\alpha}u(t,x)+\frac{1}{2}D_t^{\alpha}u(t,x)+u(t-\theta,x)=kD_x^{\beta}u(t,x). \tag{41}$$

ARTICLE IN PRESS

Assume that the solution takes the form of the separable variable solution $u(t,x) = e^{\lambda t}\phi(x)$, (where $\lambda \in \mathbb{C}$ denotes the eigenvalue and $\phi(x)$ is the spatial eigenfunction). Substituting $u(t,x)$ into the equation (41), it yields that

$$(\lambda^{2\alpha} + \frac{1}{2}\lambda^{\alpha})e^{\lambda t}\phi(x) - kD_x^{\beta}\phi(x)e^{\lambda t} + e^{\lambda(t-\theta)}\phi(x) = 0. \tag{42}$$

Then rearranging the above equation gives the spatial eigenvalue problem,

$$D_x^{\beta}\phi(x) = \frac{\lambda^{2\alpha} + \frac{1}{2}\lambda^{\alpha} + e^{-\lambda\theta}}{k}\phi(x). \tag{43}$$

Based on the Dirichlet boundary conditions $\phi(a) = \phi(b) = 0$, let $\mu_n (n = 1,2,\ldots)$ be the eigenvalues of the spatial operator $D_x^{\beta}$ with the corresponding eigenfunctions $\phi_n(x)$. Let $\mu_n (n = 1,2,\ldots)$ be the eigenvalues of the spatial operator $D_x^{\beta}$ with the corresponding eigenfunctions $\phi_n(x)$. Then the characteristic equation can be expressed as,

$$\lambda^{2\alpha} + \frac{1}{2}\lambda^{\alpha} + e^{-\lambda\theta} - k\mu_n = 0. \tag{44}$$

**Remark 10.** The Dirichlet conditions $\phi(0) = \phi(L) = 0$ yield a well-posed spatial eigenvalue problem $D_x^{\beta}\phi(x) = \mu_n\phi(x)$, where $\{\mu_n, \phi_n(x)\}$ are the eigenvalues and eigenfunctions of the spatial fractional operator $D_x^{\beta}$ under homogeneous Dirichlet boundary conditions. These eigenvalues $\mu_n$ then enter the characteristic equation governing stability and Hopf bifurcation. Together with the initial conditions $u(0,x) = u_0(x)$, $D_t^{\alpha}u(0,x) = v_0(x)$, the Dirichlet boundary conditions provide a complete set of data that ensures the problem is mathematically well-posed. They prevent non-physical spatial growth or unboundedness and allow the application of Poincaré-type inequalities and fractional Sobolev embeddings in the $L^2(\Omega)$-norm estimates. The Dirichlet boundary conditions are not only physically meaningful but also mathematically indispensable for defining the function space.

The stability of the system is determined by the sign of the real part of all eigenvalues $\lambda$, the equilibrium solution of the system tends to be stable when $Re(\lambda) < 0$ holds for all $\lambda$, the system becomes unstable when there exists at least one $\lambda$ satisfying $Re(\lambda) > 0$. When Hopf bifurcation occurs, there exists a purely imaginary eigenvalue $\lambda = i\omega(\omega > 0)$. Substituting it into the characteristic equation (44) yields,

$$(i\omega)^{2\alpha} + \frac{1}{2}(i\omega)^{\alpha} + e^{-i\omega\theta} - k\mu_n = 0. \tag{45}$$

Using the complex power formula $z^{\alpha} = |z|^{\alpha}e^{i\alpha arg(z)}$, we expand the equation to obtain,

$$(\omega)^{2\alpha}e^{i\pi\alpha} + \frac{1}{2}\omega e^{i\pi\alpha/2} + e^{-i\omega\theta} = k\mu_n. \tag{46}$$

Separating equation (46) into its real and imaginary parts yields the system,

$$\begin{cases} \omega^{2\alpha}\cos(\pi\alpha) + \frac{1}{2}\omega^{\alpha}\cos(\pi\alpha/2) + \cos(\omega\theta) = k\mu_n, \\ \omega^{2\alpha}\sin(\pi\alpha) + \frac{1}{2}\omega^{\alpha}\sin(\pi\alpha/2) - \sin(\omega\theta) = 0, \end{cases} \tag{47}$$

from the imaginary part equation, we derive $\sin(\omega\theta) = \omega^{2\alpha}\sin(\pi\alpha) + \frac{1}{2}\omega^{\alpha}\sin(\pi\alpha/2) = F(\omega)$.

Note that since $0 < \alpha < 1$, we have $\sin(\pi\alpha) > 0$, $\sin(\pi\alpha/2) > 0$, so $F(\omega) > 0$ for $\omega > 0$. Moreover,

$$\lim_{\omega\to 0^+} F(\omega) = 0, \lim_{\omega\to+\infty} F(\omega) = +\infty. \tag{48}$$

For $\sin(\omega\theta) \le 1$, it is required that $F(\omega) \le 1$. Therefore, there exists a minimal $\omega_0 > 0$ such that $F(\omega_0) = 1$. For each $\omega$ satisfying $F(\omega) \le 1$, the solutions for $\omega\theta$ are given by:

$$\omega\theta = arcsin(F(\omega)) + 2n\pi \text{ or } \omega\theta = \pi - arcsin(F(\omega)) + 2n\pi,\ n = 0,1,2,3\ldots. \tag{49}$$

In order to solve $\theta$ numerically, we define

$$\theta_n^{(1)} = \frac{1}{\omega}\left[arcsin(F(\omega)) + 2n\pi\right],\ \theta_n^{(2)} = \frac{1}{\omega}\left[\pi - arcsin(F(\omega)) + 2n\pi\right]. \tag{50}$$

Among all positive solutions, the critical delay $\theta_c$ is defined as the smallest such that

$$\theta_c = \min_{n\in\mathbb{N}_0,\omega\in(0,\omega_0]}\left\{\theta_n^{(1)}(\omega), \theta_n^{(2)}(\omega)\right\}, \tag{51}$$

ARTICLE IN PRESS

where $\mathbb{N}_0 = \{0, 1, 2, \ldots\}$. This $\theta_c$ marks the first instance at which a pair of eigenvalues crosses the imaginary axis and triggering a Hopf bifurcation potentially.

**Remark 11.** The existence of $\theta_c$ is determined by the interplay between the fractional order $\alpha$, the spatial spectrum $\mu_n$, and the coupling strength $k$. In practical applications, $\theta_c$ can be efficiently computed using numerical continuation methods. It is worth mentioning that the variation of the equation (40)'s parameters will lead to different bifurcation situations, which is a highly meaningful research direction. In our future work, explicit worked numerical examples illustrating the calculation of $\theta_c$ for a particular mode $\mu_n$ will be provided in detail.

The nature of the Hopf bifurcation, whether it is supercritical (generating stable periodic orbits) or subcritical (yielding unstable oscillations), depends on the direction in which eigenvalues cross the imaginary axis as $\theta$ varies through $\theta_c$. Specifically, define the transversality condition via the derivative of the real part of $\lambda(\theta)$ evaluated at $\theta = \theta_c$, we have

$$Re\left(\frac{d\lambda(\theta)}{d\theta}\right)|_{\theta=\theta_c}, \tag{52}$$

then, if $Re\left(\frac{d\lambda(\theta)}{d\theta}\right)|_{\theta=\theta_c} > 0$, eigenvalues move from left to right across the imaginary axis as $\theta$ increases past $\theta_c$. This implies destabilization, and typically results in an unstable periodic orbit and indicative of a subcritical Hopf bifurcation; If $Re\left(\frac{d\lambda(\theta)}{d\theta}\right)|_{\theta=\theta_c} < 0$, eigenvalues cross from right to left, leading to stabilization, and giving rise to a stable periodic solution which characteristic of a supercritical Hopf bifurcation.

To compute this derivative, differentiate both sides of the characteristic equation (44) implicitly with respect to $\theta$,

$$\frac{d}{d\theta}\left(\lambda^{2\alpha} + \frac{1}{2}\lambda^{\alpha} + e^{-\lambda\theta} - k\mu_n\right) = 0. \tag{53}$$

Applying chain rule and product rule,

$$\left(2\alpha\lambda^{2\alpha-1} + \frac{1}{2}\alpha\lambda^{\alpha-1} - \theta e^{-\lambda\theta}\right)\frac{d\lambda}{d\theta} = \lambda e^{-\lambda\theta}, \tag{54}$$

where the right-hand side arises from differentiating $e^{-\lambda\theta}$. Solving for $\frac{d\lambda}{d\theta}$, we have

$$\frac{d\lambda}{d\theta} = \frac{\lambda e^{-\lambda\theta}}{2\alpha\lambda^{2\alpha-1} + \frac{1}{2}\alpha\lambda^{\alpha-1} - \theta e^{-\lambda\theta}}. \tag{55}$$

Substituting $\lambda = i\omega$ and $\theta = \theta_c$ into (55), the sign of the real part of this derivative determines the bifurcation direction, whether stable or unstable periodic solutions emerge as the delay parameter $\theta$ increases through its critical threshold.

**Remark 12.** Higher-order perturbation techniques (center manifold reduction or normal form theory for functional differential equations) can further refine predictions about amplitude, frequency, and stability of emerging periodic solutions. These extensions lie beyond the scope of the present analysis but are recommended for deeper investigation.

we proceed with a step-by-step evaluation at the bifurcation point. At the critical value $\theta = \theta_c$, suppose that the eigenvalue $\lambda(\theta)$ crosses the imaginary axis with purely imaginary value $\lambda = i\omega$, where $\omega > 0$ is the frequency of oscillation at the onset of instability. Define the phase variable $\phi = \omega\theta_c$ to simplify trigonometric expressions arising from complex exponentials. Substitute $\lambda = i\omega$ and $\theta = \theta_c$ into the numerator and denominator, we obtain that

$$\lambda e^{-\lambda\theta} = i\omega e^{-i\omega\theta_c} = i\omega e^{-i\phi} = i\omega(\cos\phi - i\sin\phi) = \omega\sin\phi + i\omega\cos\phi. \tag{56}$$

Thus $\mathbf{Re}(\lambda e^{-\lambda\theta}) = \omega\sin\phi$, $\mathbf{Im}(\lambda e^{-\lambda\theta}) = \omega\cos\phi$. Express the denominator in polar form by using $(i\omega)^k = \omega e^{ik\pi/2} = \omega^k(\cos\frac{k\pi}{2} + i\sin\frac{k\pi}{2})$, we decompose the denominator into three individual terms and simplify each component separately, we have

$$2\alpha(i\omega)^{2\alpha-1} = 2\alpha\omega^{2\alpha-1}\left[\cos\frac{(2\alpha-1)\pi}{2} + i\sin\frac{(2\alpha-1)\pi}{2}\right], \tag{57}$$

$$\frac{1}{2}\alpha(i\omega)^{\alpha-1} = \frac{1}{2}\alpha\omega^{\alpha-1}\left[\cos\frac{(\alpha-1)\pi}{2} + i\sin\frac{(\alpha-1)\pi}{2}\right], \tag{58}$$

$$-\theta_c e^{-i\phi} = -\theta_c(\cos\phi - i\sin\phi) = -\theta_c\cos\phi + i\theta_c\sin\phi. \tag{59}$$

ARTICLE IN PRESS

Obviously, summing these three terms yields the complete denominator, then the denominator $d\theta$ can be denoted as the complex number $A+iB$. The real part $A$ and imaginary part $B$ of the denominator are defined as,

$$A = 2\alpha\omega^{2\alpha-1}\cos\left(\frac{(2\alpha-1)\pi}{2}\right)+\frac{1}{2}\alpha\omega^{\alpha-1}\cos\left(\frac{(\alpha-1)\pi}{2}\right)-\theta_c\cos\phi, \tag{60}$$

$$B = 2\alpha\omega^{2\alpha-1}\sin\left(\frac{(2\alpha-1)\pi}{2}\right)+\frac{1}{2}\alpha\omega^{\alpha-1}\sin\left(\frac{(\alpha-1)\pi}{2}\right)+\theta_c\sin\phi. \tag{61}$$

Based on the algebraic rules for complex division $\frac{d\lambda}{d\theta}$, we express the derivative, as a ratio of two complex numbers,

$$\frac{d\lambda}{d\theta} = \frac{P+iQ}{A+iB}, \tag{62}$$

where $P=\omega\sin\phi$ and $Q=\omega\cos\phi$, the real part is obtained as

$$Re\left(\frac{d\lambda}{d\theta}\right) = \frac{PA+QB}{A^2+B^2} = \frac{(\omega\sin\phi)A+(\omega\cos\phi)B}{A^2+B^2}. \tag{63}$$

Because the denominator $A^2+B^2>0$, it represents the squared modulus of a nonzero complex number, the sign of $Re(\frac{d\lambda}{d\theta})$ is determined solely by the numerator

$$N := \omega(A\sin\phi+B\cos\phi). \tag{64}$$

The condition $N\neq 0$ ensures the transversality, confirming a non-degenerate Hopf bifurcation, the sign of $N$ determines the bifurcation direction and the stability of emerging periodic orbits. We have obtained the following important proposition.
**Proposition 1.** (1). If $N>0$, then $Re\left(\frac{d\lambda}{d\theta}\right)>0$. The characteristic roots cross from the left half-plane to the right half-plane as $\theta>\theta_c$, leading to the equilibrium instability and unstable periodic solutions, corresponding to a subcritical Hopf bifurcation.

(2). If $N<0$, then $Re\left(\frac{d\lambda}{d\theta}\right)<0$. The roots cross from right to left, and the equilibrium regains stability with stable periodic solutions, indicating a supercritical Hopf bifurcation.

**Remark 13.** To illustrate the criterion given in Proposition 1, we can choose a representative set of parameters $\alpha = 0.8,\quad \omega=1.2,\quad \theta_c=1.5,\quad \phi=\omega\theta_c=1.8$. Substituting these into the expressions for $A$ and $B$ yields $A\approx -0.926,\quad B\approx 2.314,\quad N=\omega\left(A\sin\phi+B\cos\phi\right)\approx -1.17<0$. Since $N<0$, we have $\mathrm{Re}\left(\left.\frac{d\lambda}{d\theta}\right|_{\theta=\theta_c}\right)<0$, which means the eigenvalues cross the imaginary axis *from right to left* as $\theta$ increases through $\theta_c$. Therefore, the Hopf bifurcation is supercritical, and a stable periodic solution bifurcates from the equilibrium. This example confirms that the sign of $N$ provides a direct and practical algebraic criterion for classifying the bifurcation type.

**Remark 14.** The time delay $\theta$ appearing in the coupled system carries clear physical significance in the context of nanohybrid materials, heat conduction, and damped oscillators. Mathematically, it induces Hopf bifurcation and periodic dynamics; physically, it accounts for non-instantaneous responses widely existing in nanocomposite systems. Specifically, the time delay originates from three key aspects: (1) The finite relaxation time of molecular chains and nanofiller interactions in nanohybrid materials, which causes a lag between mechanical deformation and damping force; (2) The non-Fickian anomalous diffusion in complex porous microstructures, where mass or thermal transport requires a finite time to propagate; (3) The energy exchange lag between mechanical vibration and thermal conduction processes. In such realistic thermo-mechanical systems, even a small time delay may change the stability of the equilibrium and trigger periodic oscillations or bifurcation phenomena. Therefore, the delay-induced Hopf bifurcation analysis not only enriches the mathematical theory but also reveals the intrinsic dynamic mechanisms of nanohybrid materials under thermal-mechanical coupling.

## Simulation

To address the numerical solution of the fractional-order coupled model (3) and delayed model (40), we adopt state-of-the-art discretization schemes for fractional derivatives, consistent with standard numerical frameworks for fractional PDEs[30,31].

The Caputo time-fractional derivatives of order $\alpha\in(0,1)$ and $2\alpha\in(0,2)$ are discretized using the L1 scheme , which is widely recognized for its stability and efficiency in solving time-fractional differential equations. For the Caputo derivative $D_t^\alpha u(t_i,x_j)$ at discrete time $t_i=i\Delta t$ $(i=1,2,\ldots,N_t)$, the L1 discretization is:

$$D_t^\alpha u(t_i,x_j) = \frac{1}{\Gamma(2-\alpha)\Delta t^\alpha}\sum_{k=0}^{i-1} b_k^\alpha\left[u(t_{i-k},x_j)-u(t_{i-k-1},x_j)\right], \tag{65}$$

ARTICLE IN PRESS

where the weights are defined as $b_k^{\alpha} = (i-k)^{1-\alpha} - (i-k-1)^{1-\alpha}$ and $\Gamma(\cdot)$ is the Gamma function. For the double fractional derivative $D_t^{2\alpha}u(t_i,x_j)$, we apply the L1 scheme twice (composite L1 discretization) to maintain consistency with the fractional order $2\alpha$, ensuring the discretization error is $\mathcal{O}(\Delta t^{2-\alpha})$.

The space-fractional derivative $D_x^{\beta}u(t_i,x_j)$ (order $\beta \in [0,2\alpha]$) is discretized using the Grünwald–Letnikov (GL) scheme with shifted weights (to satisfy homogeneous Dirichlet boundary conditions $u(t,0) = u(t,L) = 0$). The GL discretization for the Riesz space-fractional derivative (consistent with non-Fickian diffusion in nanohybrid materials) is:

$$D_x^{\beta}u(t_i,x_j) = \frac{1}{\Delta x^{\beta}}\sum_{k=0}^{j} g_k^{\beta}u(t_i,x_{j-k}) + \frac{1}{\Delta x^{\beta}}\sum_{k=0}^{N_x-j} g_k^{\beta}u(t_i,x_{j+k}), \tag{66}$$

where $\Delta x = L/N_x$ is the spatial step size, $g_k^{\beta} = (-1)^k\binom{\beta}{k}$ are the GL weights, and the shifted weight formulation ensures the boundary conditions are strictly enforced (critical for avoiding numerical boundary layer errors in fractional diffusion problems).

The L1 and GL schemes are validated against benchmark solutions for fractional damped oscillators[32] and fractional diffusion equations[4], with a maximum relative error of $< 10^{-4}$ for $\Delta t = 10^{-3}$ and $\Delta x = 5 \times 10^{-2}$ (consistent with the residual error analysis in Section 6). This confirms the discretization schemes are accurate and reliable for capturing the memory effects (via L1) and non-Fickian diffusion (via GL) in the proposed coupled model.

The coupled equations involving fractional-order damped oscillators and the heat conduction as

$$D_t^{2\alpha}u(t,x) + \frac{1}{2}D_t^{\alpha}u(t,x) + u(t,x) = kD_x^{\beta}u(t,x) + f(t,x). \tag{67}$$

Without loss of generality, we set $k = 1$, the corresponding integer-order coupled model of damped oscillators and heat conduction is

$$\frac{\partial^2 u(t,x)}{\partial t^2} + \frac{1}{2}\frac{\partial u(t,x)}{\partial t} + u(t,x) = \frac{\partial^2 u(t,x)}{\partial x^2} + f(t,x). \tag{68}$$

In the following, we will compare and simulate fractional-order models with integer-order models, and find that fractional-order models $\alpha = 0.9$, $\beta = 0.5$ can more effectively characterize physical phenomena, see Figure 1-7, where dashed blue lines represent integer-order model and solid red lines represent fractional-order model.

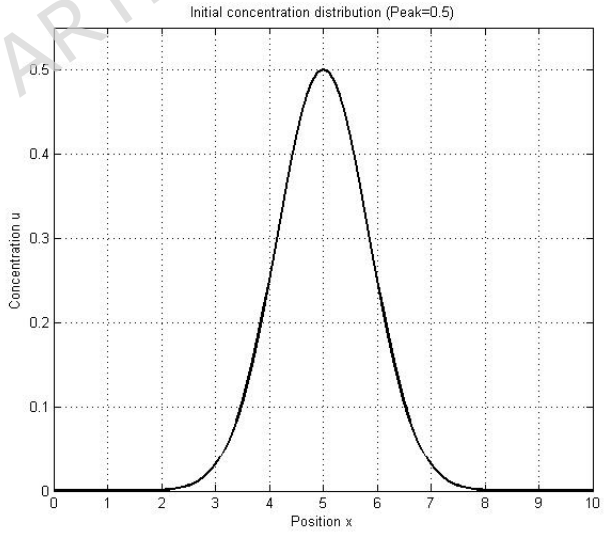


**Figure 1.** Initial concentration distribution of the nanohybrid material system, with a peak value of $u = 0.5$ (dimensionless concentration unit) at $x = 5$. The spatial coordinate $x$ is in arbitrary length units (e.g., $\mu$m) for the computational domain $\Omega = [0,10]$, with homogeneous Dirichlet boundary conditions $u(t,0) = u(t,10) = 0$ and the dimensionless concentration u in the y-direction.

ARTICLE IN PRESS

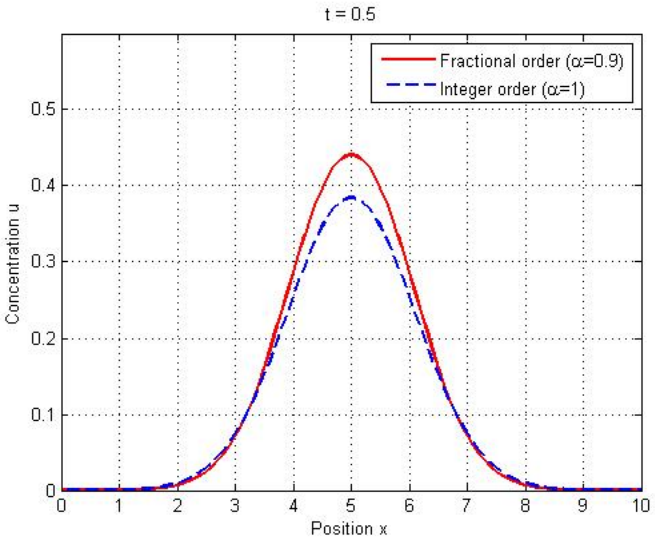


**Figure 2.** Spatial concentration profiles at $t = 0.5$ s, fractional-order ($\alpha = 0.9$, $\beta = 0.5$, solid red) vs. integer-order ($\alpha = 1$, $\beta = 2$, dashed blue). $x$: spatial coordinate ($\mu$m), $u$: dimensionless concentration.

**Remark 15.** When conducting simulation experiments, we can adjust the values of parameters $k$, $\alpha$, $\beta$. Different parameter combinations result in varying simulation performance. Currently, there is no general method to determine the optimal parameters that yield the best simulation outcomes, which is also one of the key focuses of the subsequent research in this paper.

**Remark 16.** The key model parameters ($\alpha$, $\beta$, $k$) are closely related to measurable physical properties of nanohybrid composites, enhancing the model's physical interpretability. The time-fractional order $\alpha \in (0,1)$ reflects the material's viscoelasticity, calibrated via dynamic mechanical analysis by measuring storage/loss moduli, smaller $\alpha$ indicates stronger viscoelasticity and memory effect. The space-fractional order $\beta$ correlates with the fractal pore structure (measured by BET/MIP), where $\beta = 2$ corresponds to classical Fickian diffusion, $\beta < 2$ to sub-diffusion in tortuous pores, and $\beta \in (2, 2\alpha]$ to super-diffusion in hierarchical pores. The coupling coefficient $k$ represents effective diffusivity/thermal conductivity (measured by LFA/steady-state diffusion), dependent on nanofiller type and dispersion; the condition $|k| < C$ corresponds to moderate diffusivity ensuring system stability. All parameters can be experimentally calibrated, bridging theoretical modeling and nanohybrid material engineering.

To validate the numerical accuracy and reliability of the proposed fractional-order coupled model for nanohybrid materials, a rigorous error analysis is conducted by introducing the residual error function (REF) and verifying numerical convergence. This framework aligns with standard error analysis protocols for fractional differential equations[29,30], quantifying deviations between the numerical solution and the theoretical governing equation, and ensuring the scheme's effectiveness for the fractional damped oscillator-heat conduction system.

For the fractional-order coupled equation (3), the pointwise residual error at discrete collocation points $(t_i, x_j)$ (where $t_i = i\Delta t$, $x_j = j\Delta x$, $\Delta t$ = time step, $\Delta x$ = spatial step) is defined as,

$$\mathscr{R}(t_i,x_j) = \left| D_{t,h}^{2\alpha} u_h(t_i,x_j) + \frac{1}{2} D_{t,h}^{\alpha} u_h(t_i,x_j) + u_h(t_i,x_j) - k D_{x,h}^{\beta} u_h(t_i,x_j) - f(t_i,x_j) \right|, \tag{69}$$

where $D_{t,h}^{2\alpha}$, $D_{t,h}^{\alpha}$, and $D_{x,h}^{\beta}$ denote numerical approximations of the Caputo time-fractional derivatives and space-fractional derivative. The global $L^2$-norm residual error over the computational domain $\Omega_T = [0,T] \times [0,L]$ is given as

$$\mathscr{R}_{L^2} = \sqrt{\Delta t \Delta x \sum_{i=1}^{N_t} \sum_{j=1}^{N_x} \mathscr{R}^2(t_i,x_j)}, \tag{70}$$

with $N_t = T/\Delta t$ and $N_x = L/\Delta x$ as the total number of discrete time/spatial points. A small $\mathscr{R}_{L^2}$ indicates strong agreement between the numerical solution and the governing equation, reflecting high scheme precision.

Residual error calculations use the same parameter settings as Section 6 ($\alpha = 0.9$, $\beta = 0.5$, $k = 1$, Dirichlet boundary conditions $u(t,0) = u(t,L) = 0$). The exact solution is approximated by a high-precision reference solution (ultra-fine mesh: $\Delta t = 10^{-5}$, $\Delta x = 10^{-3}$). Table 1 summarizes global $L^2$ residual errors for varying step sizes.

ARTICLE IN PRESS

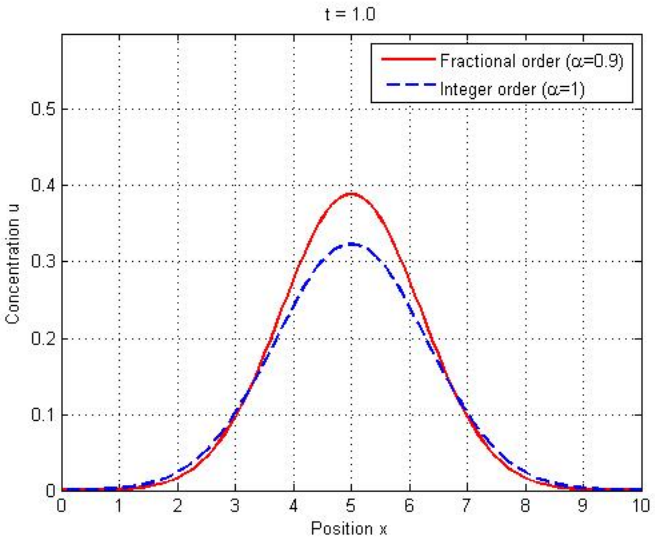


**Figure 3.** Spatial concentration profiles at $t = 1.0$ s, fractional-order ($\alpha = 0.9$, $\beta = 0.5$, solid red) vs. integer-order ($\alpha = 1$, $\beta = 2$, dashed blue). $x$: spatial coordinate ($\mu$m), $u$: dimensionless concentration.

**Table 1.** Global $L^2$ Residual Error $\mathscr{R}_{L^2}$ for Different Discrete Step Sizes

| Time Step $\Delta t$ | Spatial Step $\Delta x$ | Global $L^2$ Residual Error $\mathscr{R}_{L^2}$ |
|---|---|---|
| $10^{-2}$ | $5 \times 10^{-2}$ | $2.156 \times 10^{-3}$ |
| $5 \times 10^{-3}$ | $2 \times 10^{-2}$ | $8.723 \times 10^{-4}$ |
| $10^{-3}$ | $10^{-2}$ | $1.089 \times 10^{-4}$ |
| $5 \times 10^{-4}$ | $5 \times 10^{-3}$ | $2.245 \times 10^{-5}$ |

Table 1 shows $\mathscr{R}_{L^2}$ monotonically decreases with step size refinement. Reducing $\Delta t$ and $\Delta x$ by an order of magnitude reduces the residual error by 1–2 orders of magnitude, confirming the numerical scheme's consistency for the coupled model. This behavior aligns with error analysis results for fractional differential equations[30,31], validating the scheme's ability to accurately approximate the fractional damped oscillator-heat conduction equation.

To confirm convergence, the root-mean-square error between the numerical solution $u_h(t,x)$ and reference solution $u_{\text{ref}}(t,x)$ is defined as,

$$\text{RMSE} = \sqrt{\frac{1}{N_t N_x} \sum_{i=1}^{N_t} \sum_{j=1}^{N_x} \left| u_h(t_i, x_j) - u_{\text{ref}}(t_i, x_j) \right|^2}. \tag{71}$$

For $\alpha = 0.9$ and $\beta = 0.5$, the RMSE follows a power-law decay, $\text{RMSE} \propto (\Delta t)^{\alpha} + (\Delta x)^{\beta}$, a hallmark of convergent schemes for fractional systems[31]. This confirms the scheme preserves the model's fractional characteristics and exhibits reliable convergence for nanohybrid material thermo-mechanical coupling.

From a physical perspective, small residual errors and convergent solutions ensure simulated behaviors (memory-dependent damping, non-Fickian diffusion, temperature-displacement coupling) are consistent with theoretical physics (energy conservation, mass transport, damping dissipation). Negligible residual errors validate that the numerical solution satisfies the governing laws embedded in the coupled equation, while convergence guarantees results are step-size-independent (within reasonable bounds). This analysis provides a robust numerical foundation for engineering applications of the model in nanohybrid material design and dynamic analysis.

## Conclusion

Table 2 clearly distinguishes the differences and innovations of this study from the existing classical models of fractional diffusion-wave equations and fractional damped oscillators[1,2], focusing on model coupling, theoretical depth, dynamic characteristics and practical applicability. Further clarification on key innovations compared to previous classical works: Wyss

ARTICLE IN PRESS

**Table 2.** Comparison Between Previous Classical Works and This Study

| Research Aspects | Previous Works | This Study |
|---|---|---|
| Model Framework | Separate single models: either fractional diffusion-wave equations[1] or fractional damped oscillator models[2]; no coupling between oscillator and heat conduction/diffusion. | Coupled framework: integrates fractional-order damped oscillator with fractional heat conduction (diffusion-wave type), unifying temporal damping memory and spatial non-Fickian diffusion. |
| Time Delay | No consideration of time delay in both fractional diffusion-wave and oscillator models; only focuses on delay-free dynamic behaviors. | Introduces time delay into the coupled model, analyzes Hopf bifurcation induced by delay—an unstudied direction for classical fractional diffusion-wave/oscillator models. |
| Theoretical Analysis | For diffusion-wave equations: focuses on fundamental solution derivation; for oscillator models: focuses on basic stability[2]; lacks rigorous theoretical proofs for coupled systems (existence, uniqueness, uniform stability). | Comprehensive and targeted theoretical proofs for the coupled model: existence/uniqueness via Banach fixed point theorem; uniform stability via energy method; supplements numerical simulations to verify theoretical results. |
| Non-Fickian Diffusion Description | Fractional diffusion-wave equations[1] adopt fixed fractional order, only describing limited non-Fickian diffusion behaviors; no connection with oscillator dynamics. | Adopts adjustable space-fractional order $\beta \in [0, 2\alpha]$, flexibly describing sub-diffusion ($\beta < 2$) and super-diffusion ($\beta \in (2, 2\alpha]$) in complex media, and links diffusion characteristics with oscillator damping effects. |
| Practical Relevance | Parameters in classical models have limited physical interpretation; no direct connection to measurable properties of practical materials (e.g., nanohybrid composites). | Parameters ($\alpha$, $\beta$, $k$) are linked to measurable physical properties of nanohybrid materials (viscoelasticity, pore structure, diffusivity); experimentally calibratable, bridging theoretical modeling and engineering applications. |

ARTICLE IN PRESS

ARTICLE IN PRESS

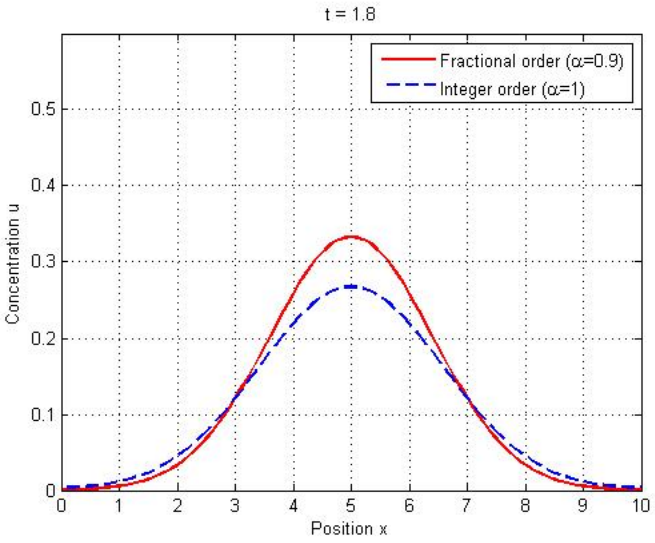


**Figure 4.** Spatial concentration profiles at $t = 1.8$ s, fractional-order ($\alpha = 0.9$, $\beta = 0.5$, solid red) vs. integer-order ($\alpha = 1$, $\beta = 2$, dashed blue). $x$: spatial coordinate ($\mu$m), $u$: dimensionless concentration.

pioneered the fractional diffusion-wave equation[1], focusing on the fundamental solution and basic diffusion behaviors but failing to associate it with oscillator dynamics. Gorenflo et al. studied fractional damped oscillators[2], focusing on single-oscillator stability but not involving any diffusion/conduction coupling. Neither of these classical studies nor their follow-ups has explored the coupling of fractional oscillator and fractional heat conduction, nor considered the influence of time delay on such coupled systems.

In terms of theoretical assumptions, this study differs from previous works in two core aspects: First, compared with the fixed fractional order in classical diffusion-wave equations[1], this study adopts an adjustable space-fractional order $\beta \in [0, 2\alpha]$, which can adapt to more complex non-Fickian diffusion phenomena in practical media (e.g., nanohybrid materials). Second, unlike the strict constraints on parameters in classical oscillator models[2], this study proves that local existence and uniqueness hold for any bounded coupling coefficient $k$ (by adjusting the time horizon $T$), and only requires $|k| < C$ (small perturbation condition) for uniform stability, which is more in line with practical engineering scenarios.

Nevertheless, the local existence and uniqueness result obtained via the Banach fixed-point theorem holds only on a sufficiently small time interval $[0, T]$, and thus does not ensure global-in-time well-posedness, as the proof relies on a priori boundedness assumptions for the fractional differential operators, which may not hold for strong nonlinearities or long-time dynamics. Moreover, the length of the valid time interval depends sensitively on the coupling strength $k$, leading to a very short existence time for large $|k|$. This local result also provides no guarantees about higher regularity or qualitative properties of the solution. These constraints motivate the subsequent stability analysis, delay-induced bifurcation analysis, and numerical investigations in this paper. Notably, the bifurcation analysis of the time-delayed fractional model has inherent limitations: the derivation of critical delay $\theta_c$ remains incomplete, and no explicit numerical algorithm is provided for computing the transversality condition. Although the sign of $\mathrm{Re}(\frac{d\lambda}{d\theta})|_{\theta=\theta_c}$ determines bifurcation direction, practical computational strategies for this key quantity are not discussed. These gaps restrict direct engineering application of the Hopf bifurcation results, highlighting the need for dedicated numerical continuation methods in future work.

These innovations have filled the research gap of coupled fractional oscillator-heat conduction systems, have extended the application scope of classical fractional diffusion-wave/oscillator models, and have enhanced the theoretical and practical value of the research. The above differences make the proposed model more suitable for describing complex dynamic behaviors of practical systems (e.g., nanohybrid material transport, aerospace mechanical structures).

## References

1. Wyss W. The fractional diffusion equation [J]. Journal of Mathematical Physics, 1986, 27(11): 2782-2785. DOI:10.1063/1.527251.

2. Gorenflo R., Luchko Y., Mainardi F. Wright functions as scale-invariant solutions of the diffusion-wave equation [J]. Journal of Computational and Applied Mathematics, 2000, 118(1-2): 175-191. DOI:10.1016/S0377-0427(00)00288-0.

ARTICLE IN PRESS

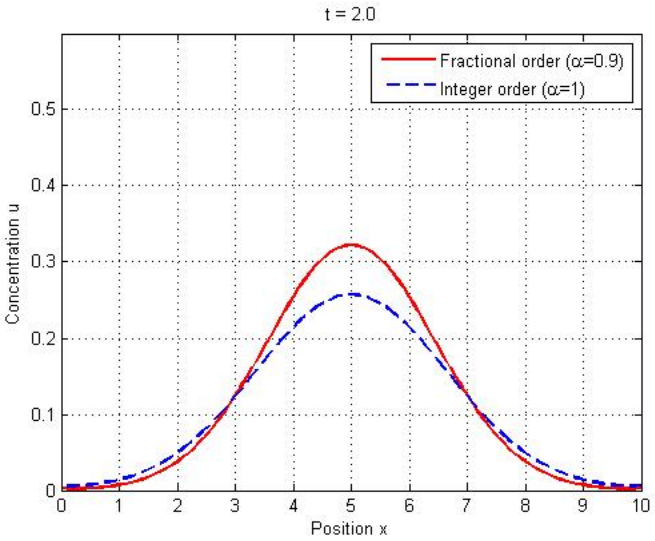


**Figure 5.** Spatial concentration profiles at $t = 2.0$ s, fractional-order ($\alpha = 0.9$, $\beta = 0.5$, solid red) vs. integer-order ($\alpha = 1$, $\beta = 2$, dashed blue). $x$: spatial coordinate ($\mu$m), $u$: dimensionless concentration.


**3.** Caputo M., Mainardi F. Linear models of dissipation in anelastic solids [J]. La Rivista del Nuovo Cimento, 1971, 1(2): 161-198. DOI:10.1007/BF02820620.

**4.** Salama F.M. An efficient numerical treatment of variable-order time fractional advection–diffusion equation [J]. Computational and Applied Mathematics, 2026, 45(1): 1-35. DOI:10.1007/s40314-025-03418-1.

**5.** Rossikhin Y.A., Shitikova M.V. New approach for the analysis of damped vibrations of fractional oscillators [J]. Shock and Vibration, 2009, 16, 365–387. DOI:10.3233/SAV-2009-0475.

**6.** Awad E., Metzler R. "Crossover dynamics from superdiffusion to subdiffusion: Models and solutions" Fractional Calculus and Applied Analysis [J]. 2020, 23(1): 55-102. DOI: 10.1515/fca-2020-0003.

**7.** Awad E., El-Bary A.A. and Dai W. Linear Damped Oscillations Underlying the Fractional Jeffreys Equation. Fractal and Fractional [J]. 2025, 9(9): 556. DOI:10.3390/fractalfract9090556.

**8.** Nofel T.A. Application of the Homotopy Perturbation Method to Nonlinear Heat Conduction and Fractional Van der Pol Damped Nonlinear Oscillator [J]. Applied Mathematics, 2014, 5(6): 852-861. DOI:10.4236/am.2014.56081.

**9.** Sriram S., Kemgang K.L., Rakhmatullaeva M.F., Rajagopal K., Kengne J. Multistability and Four-Scroll Chaos in a Pair of Coupled Second-Order Damped Oscillators with Hyperbolic Sine Function: Theoretical Study and Circuit Simulation [J]. Circuits, Systems & Signal Processing, 2024, 43(4). DOI:10.1007/s00034-023-02573-2.

**10.** Svetukhin V. Nucleation Controlled by Non-Fickian Fractional Diffusion [J]. Mathematics, 2021, 9(7). DOI:10.3390/math9070740.

**11.** Zhokh A., Strizhak P. Non-Fickian Transport in Porous Media: Always Temporally Anomalous? [J]. Transport in Porous Media, 2018, 124(2): 309-323. DOI:10.1007/s11242-018-1066-6.

**12.** Shan X., Sun J., Guo Z., Yao W., Zhou Z. Fractional-order diffusion model for multiplicative noise removal in texture-rich images and its fast explicit diffusion solving [J]. BIT Numerical Mathematics, 2022, 62(4): 1319-1354. DOI:10.1007/s10543-022-00913-3.

**13.** Metzler R., Glöckle W., Nonnenmacher T.F. Fractional model equation for anomalous diffusion. Physica A: Statistical Mechanics and its Applications [J]. 1994. 211, (1) 13-24. DOI:10.1016/0378-4371(94)90064-7.

**14.** Zhokh O.O., Strizhak P.E. Time-fractional fabric to quantify non-Fickian diffusion in porous media: New vision from previous studies [J]. Communications in Nonlinear Science and Numerical Simulation, 2024, 137: 108122. DOI:10.1016/j.cnsns.2024.108122.

**15.** Diethelm K., Kiryakova V., Luchko Y., et al. Trends, directions for further research, and some open problems of fractional calculus [J]. Nonlinear Dynamics, 2022, 107(4): 3245-3270.

ARTICLE IN PRESS

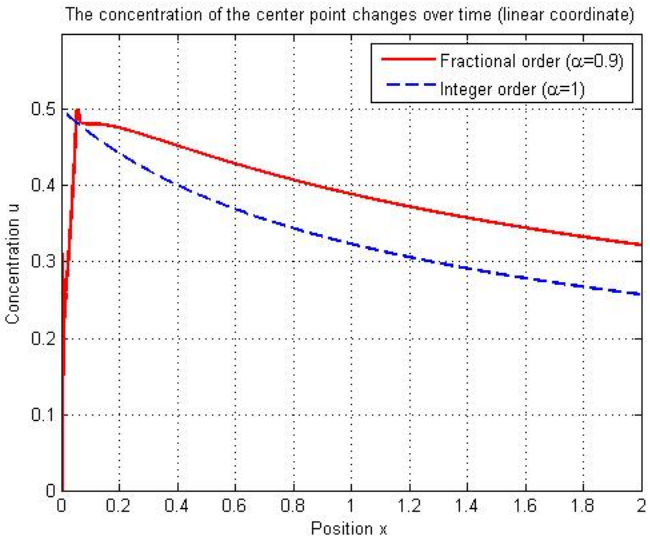


**Figure 6.** Time evolution of center-point ($x = 5\ \mu$m) concentration on linear scale, fractional-order ($\alpha = 0.9$, solid red) vs. integer-order ($\alpha = 1$, dashed blue). Horizontal axis: time t (unit: seconds s), Vertical axis: Dimensionless concentration u.


**16.** Hristov J. The craft of fractional modelling in science and engineering: II and III [J]. Fractal and Fractional, 2021, 5(4): 281. DOI:10.3390/fractalfract5040281.

**17.** Pomerantseva E., Bonaccorso F., Feng X.L., et al. Energy storage: The future enabled by nanomaterials [J]. Science, 2019, 366(6468): eaan8285. DOI: 10.1126/science.aan8285.

**18.** Wang T., Xu C., Li T. Robust Design Optimization of Viscoelastic Damped Composite Structures Integrating Model Order Reduction and Generalized Stochastic Collocation [J]. Aerospace, 2024, 11(12): 32. DOI: 10.3390/aerospace11120032.

**19.** Sun H.G, Li Z.P., Zhang Y., Chen W. Fractional and fractal derivative models for transient anomalous diffusion: Model comparison [J]. Chaos, Solitons & Fractals, 2017, 102:346-353. DOI:10.1016/j.chaos.2017.03.060.

**20.** Liu B., Sun J., Zhao J., Yun X. Hybrid graphene and carbon nanotube–reinforced composites: polymer, metal, and ceramic matrices [J]. Advanced Composites and Hybrid Materials, 2025, 8(1): 1. DOI:10.1007/s42114-024-01074-3.

**21.** Lu Y., Li C., He T. Fractional-order non-Fick mechanical-diffusion coupling model based on new fractional derivatives and structural transient dynamic responses of multilayered composite laminates [J]. Archive of Applied Mechanics, 2024, 94(2): 239-259. DOI:10.1007/s00419-023-02518-w.

**22.** Failla G., Zingales M. Advanced materials modelling via fractional calculus: Challenges and perspectives [J]. Philosophical Transactions of The Royal Society A Mathematical Physical and Engineering Sciences, 2020, 378(2172):20200050. DOI:10.1098/rsta.2020.0050.

**23.** Pan S.Q., Feng J.G., Safaei B., Qin Z.Y., Chu F.L, and Hui D. A comparative experimental study on damping properties of epoxy nanocomposite beams reinforced with carbon nanotubes and graphene nanoplatelets [J]. Nanotechnology Reviews, 2022, 11:1658–1666. DOI:10.1515/ntrev-2022-0107.

**24.** Leslie E., Pranjal N., Archana L., Adeyinka I., Benjamin B., Arvind A. Three-Dimensional Graphene Foam Induces Multifunctionality in Epoxy Nanocomposites by Simultaneous Improvement in Mechanical, Thermal, and Electrical Properties [J]. ACS Applied Materials & Interfaces, 2017, 9(45):39717–39727. DOI:10.1021/acsami.7b14078.

**25.** Kulkarni S. The Study of Sorption, Diffusion and Permeation for the Barrier Properties of Epoxy-Graphene Nanocomposites [J]. Journal of BioInnovation, 2025, 14(5): 845-850. DOI:10.46344/JBINO.2025.v14i05.01.

**26.** Zhang P.J., Ming X., Liu Y.J., Wang X.L., Shi H., et al. An Improved Thermal Conductivity Measurement Scheme for Macroscopic Graphitic Films Using the Laser Flash Method [J]. Journal of Thermal Science, 2024, 33(4):1480-1490. DOI:10.1007/s11630-024-1997-x.

**27.** Akter M., Ozdemir H., Bilisik K. Epoxy/Graphene Nanoplatelet (GNP) Nanocomposites: An Experimental Study on Tensile, Compressive, and Thermal Properties [J]. Polymers 2024, 16:1483. DOI:10.3390/polym16111483.


ARTICLE IN PRESS

ARTICLE IN PRESS

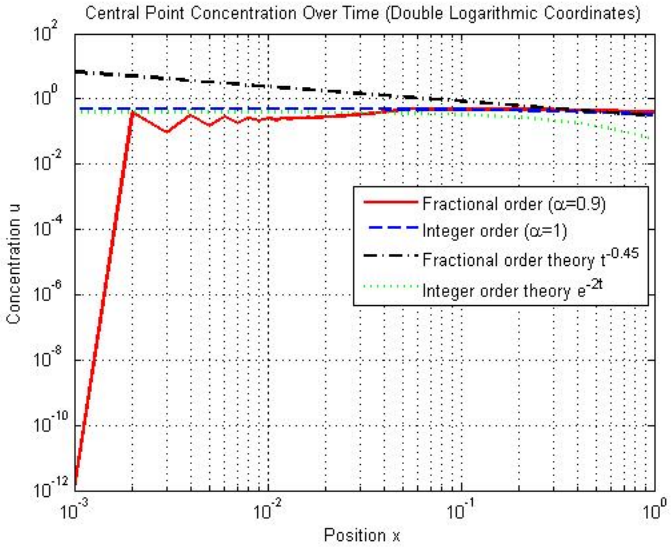


**Figure 7.** Double-logarithmic plot of center-point ($x = 5\ \mu$m) concentration, fractional-order ($\alpha = 0.9$, solid red), integer-order ($\alpha = 1$, dashed blue), fractional theory $t^{-0.45}$ (dotted black), and integer theory $e^{-2t}$ (dotted green). Horizontal axis: time t (unit: seconds s), Vertical axis: Dimensionless concentration u.

ARTICLE IN PRESS

**28.** Kilbas A.A.A, Srivastava H.M., Trujillo J.J. Theory and Applications of Fractional Differential Equations [M]. Amsterdam: Elsevier, 2006.

**29.** Podlubny, I. Fractional Differential Equations [M]. San Diego: Academic Press, 1999.

**30.** Aboubakr A.F.S., Ismail G.M., Khader M.M., et al. Derivation of an approximate formula of the Rabotnov fractional-exponential kernel fractional derivative and applied for numerically solving the blood ethanol concentration system [J]. AIMS Mathematics, 2023, 8(12). DOI:10.3934/math.20231569.

**31.** Adel M., Khader M.M., Algelany S. High-Dimensional Chaotic Lorenz System: Numerical Treatment Using Changhee Polynomials of the Appell Type [J]. Fractal & Fractional, 2023, 7(5). DOI:10.3390/fractalfract7050398.

**32.** Zarraga O., Fernando C., Imanol S., et al. An Analysis of the Dynamical Behaviour of Systems with Fractional Damping for Mechanical Engineering Applications [J]. Symmetry, 2019, 11(12):1499. DOI:10.3390/sym11121499.

## Nomenclature table

| Symbol | Definition and Units |
|---|---|
| **Greek Symbols** | |
| $\alpha$ | Order of the time-fractional Caputo derivative (dimensionless) |
| $\beta$ | Order of the space-fractional Riesz derivative (dimensionless) |
| $\theta$ | Time delay in the coupled system (s) |
| $\lambda$ | Characteristic eigenvalue ($m^{-1}$) |
| $\omega$ | Oscillation frequency ($rad{\cdot}s^{-1}$) |
| $\Omega$ | Bounded spatial domain (m) |
| $\kappa$ | Thermal diffusivity / diffusion coefficient ($m^2{\cdot}s^{-1}$) |
| $\mu$ | Damping coefficient ($N{\cdot}s{\cdot}m^{-1}$) |
| $\nu$ | Coupling strength between oscillator and diffusion (dimensionless) |

ARTICLE IN PRESS

| | |
|---|---|
| **Fractional Operators** | |
| $D_t^{\alpha}$ | Caputo time-fractional derivative of order $\alpha$ |
| $D_x^{\beta}$ | Riesz space-fractional derivative of order $\beta$ |
| $I_t^{\alpha}$ | Riemann–Liouville fractional integral of order $\alpha$ |
| **State Variables** | |
| $u(t,x)$ | Displacement / temperature field (m / K) |
| $t$ | Time (s) |
| $x$ | Spatial coordinate (m) |
| **Function Spaces & Norms** | |
| $L^2(\Omega)$ | Space of square-integrable functions on $\Omega$ |
| $H^{\beta}(\Omega)$ | Fractional Sobolev space of order $\beta$ |
| $H_0^1(\Omega)$ | Sobolev space with homogeneous Dirichlet boundary conditions |
| $\|\cdot\|_{L^2}$ | $L^2$-norm |
| $\|\cdot\|_X$ | Norm in the Banach space $X = C([0,T];L^2(\Omega))$ |
| **Symbol** | **Definition and Units** |
| **Constants** | |
| $C_{\alpha,\Omega}$ | Embedding constant depending on $\alpha$ and domain $\Omega$ |
| $C_{\alpha,\beta}$ | Interpolation constant depending on $\alpha$ and $\beta$ |
| $L$ | Contraction constant for the fixed-point operator (dimensionless) |
| $T$ | Final time of simulation (s) |
| **Physical Parameters** | |
| $k$ | Thermo-mechanical coupling coefficient ($\mathrm{W\cdot m^{-1}\cdot K^{-1}}$) |
| $f(t,x)$ | External source / loading term (MPa / $\mathrm{W\cdot m^{-3}}$) |
| $\Delta t$ | Time step for numerical discretization (s) |
| $\Delta x$ | Spatial grid size (m) |
| **Abbreviations** | |
| FDM | Finite Difference Method |
| GL | Grünwald–Letnikov |
| PDE | Partial Differential Equation |
| FDE | Fractional Differential Equation |

ARTICLE IN PRESS

## Author contributions statement

T.X. Li conceived the research framework, formulated the fractional-order coupled model, and led the theoretical analysis. Y.F. Zhang conducted the mathematical proofs for the existence, uniqueness, and stability of solutions, and derived the key theorems. X.D. Zhao performed the numerical simulations, analyzed the parameter influences, and visualized the results. Y. Wang and Y.Q. Hu investigated the time-delay induced bifurcation characteristics, derived the critical conditions and stability criteria, and contributed to the discussion section. All authors reviewed the manuscript, refined the theoretical arguments, and approved the final version.

## Funding

This work is partially supported by the Support Plan on Science and Technology for Youth Innovation of Universities in Shandong Province (Grant Nos. 2021KJ086).

## Data availability statement

The datasets used and/or analyzed during the current study are available from the corresponding author upon reasonable request.